# UFP and BC at a mid-sized city in Po valley, Italy: size-resolved partitioning between primary and newly formed particles

F. Wang[1,2], S. Cernuschi[1], S.Ozgen[1], G. Ripamonti[1], R. Vecchi[3], G. Valli[3], G. Lonati[1,*]

[1] *Department of Civil and Environmental Engineering, Politecnico di Milano, Milan 20133, Italy*
[2] *National Climate Center, China Meteorological Administration, Beijing 100081, China*
[3]*Department of Physics, Università degli Studi di Milano and INFN Milan, Italy*
[*]corresponding author: giovanni.lonati@polimi.it

**Abstract**

In Po valley (Northern Italy) concentrations of particulate matter (PM) often exceed air quality standards, and road traffic is reported as one of the main sources of pollution. This study investigates the size resolved particle number concentration and size distribution at one rural station, one urban station and one traffic station. The measured size-resolved particle number concentration has been reduced by means of cluster analysis to four particle size fractions (cluster 1: 7-29 nm, cluster 2: 29-95 nm, cluster 3: 95-264 nm, and cluster 4: 264-10000 nm) based on their behavior in atmosphere according to common time patterns. The primary emissions from traffic are evaluated based on black carbon (BC) and size-resolved particle number concentration data, considering separately single size intervals and providing cluster-resolved information on primary and newly formed particle concentration. Particles directly emitted by vehicle exhaust exhibit similar numbers for the clusters 1 to 3 while newly formed particles mainly occurs in cluster 1. Furthermore, diurnal variation of directly emitted particles is found to closely follow the BC levels, while the trend of newly formed particles varies according to air temperature, solar radiation and particle pollution levels. The results release that in Po valley the variations of particle number levels do not always reflect the variation of road traffic emissions in urban areas as the large availability of anthropogenic precursors can favor summertime nucleation events with region-wide extension

Keywords: ultrafine particles, black carbon, cluster analysis, Po valley

## 1. Introduction

Po valley is a well-known air pollution hot-spot area where particle matter mass concentrations often exceed European air quality standards (EU Directive 2008/50/EC). Bounded by the Alps on North directions, from North-West to North-East, and by the Apennines on the South, the Po valley experiences frequent stagnant meteorological conditions. Moreover, the area is densely urbanized and anthropogenic activities such as intensive agriculture and industrial activities are widely diffused implying a high density of air pollutant sources. As a consequence, the Po valley is one of the main air pollution hot-spots in Europe (e.g.: Vecchi et al., 2004; Vecchi et al., 2009; Bernardoni et al., 2011; and references therein) with PM air quality standards not complied with not only in the largest metropolitan areas but also in small and mid-sized towns. Additionally, in recent years the concern for fine and ultrafine particles has become more and more relevant but knowledge of the relation between particle sources and ambient particle number concentration levels is still incomplete. Ultrafine particles (UFP, particle diameter $dp<0.1$ μm) are believed to be more toxic than larger particles because of their higher number and surface area per given mass, and higher deposition probability in the deep lung region (Chio et al., 2008; Hoek et al., 2010). Even though legislation is not yet regulating particle number concentration (PN) but only particle mass concentration, PN and size distribution measurements have been

implemented both in urban areas and remote sites worldwide (as reviewed by Kulmala et al., 2004; Sioutas et al., 2005; Morawska et al., 2008; Kumar et al., 2010; Fuzzi et al., 2015). PN varies over three orders of magnitude from levels as high as $10^5$ $cm^{-3}$ measured at highway roadside sites to levels around $10^2$ $cm^{-3}$ measured at remote sites. In urban environments UFPs are the dominant fraction of PN, taking 70-90% of the total PN (Putaud et al., 2010). PN in urban environment shows clear seasonal, weekly and diurnal patterns due to variation in source strength and meteorological conditions. Measurements in different urban areas worldwide have similarly reported increase in PN levels during winter caused by higher emissions from heating processes together with unfavorable atmospheric dilution conditions, such as lowered mixing height and strong atmospheric stability (Wehner and Wiedensohler 2003, Wang et al., 2011; Sabaliauskas et al., 2012). Road traffic emissions are reported to be the main source of UFP in urban areas (Hussein et al., 2005; Pey et al., 2009; Perez et al., 2010; Jonsson et al., 2011). Primary particles emitted by the exhaust of vehicles tend to exhibit a size distribution with "a nucleation mode (<30 nm)" and a "carbonaceous mode (50 to >100 nm)"(as reviewed by Morawska et al., 2008). The formation of the primary nucleation mode particle during the emission, dilution and mixing to the ambient air is favoured by vehicle technology and ambient air conditions (Kittelson et al., 2002; Ristovski et al., 2006; Ronkko et al., 2006). Primary particles in the accumulation mode range (50-200 nm) emitted by vehicles are mainly soot particles composed by carbonaceous agglomerates and adsorbed materials (Kittelson et al., 2006). The soot particles containing black carbon (BC), which accounts for more than half of $PM_{2.5}$ mass from diesel engines under load (Ban-Weiss et al., 2008), is of particular concern since it was reported to be the second largest contributor to global warming (next to $CO_2$) and alters regional precipitation and snow and cloud albedo (Ramanathan and Carmichael, 2008). Moreover, exposure to BC has been associated with health effects (Janssen et al., 2012). In the urban environment nucleation processes have been expected to be prevented by the higher presence of pre-existing particles acting as condensation surface for condensable compounds. However, in the last years a large number of studies has demonstrated that nucleation commonly occurs also in urban areas (e.g. Moore et al., 2007; Hussein et al., 2008; Fernandez-Camacho et al., 2010; Salma et al., 2011). Beside the occurrence of clearly detectable events characterized by an elevate rate of new particle formation, secondary UFP, i.e.: created in the atmosphere through complex physiochemical processes (Dunn et al., 2004; Jamriska et al., 2008; Reche et al., 2011), are reported to contribute to the total UFP concentrations in urban areas. Nevertheless, at present ultrafine particles are not considered in air quality legislation so that regularly monitoring are scarce and the available knowledge on urban UFP appears still lacking compared with the complexity and variability of the phenomenon.
Such a lack of information is particularly evident for the Po valley: actually, the few studies on UFP reported in literature are mainly focused on Milan area (Rodriguez et al., 2007; Lonati et al., 2011; Ozgen et al., 2016) and information on other cities is very limited, especially as far as both BC and UFP are concerned. Therefore, in this study, we (i) characterize the spatial variability of PN at urban background and traffic-exposed sites in a mid-sized city, as well as at a nearby rural site, located in the heavily polluted Po valley; (ii) investigate the relationship between BC aerosol mass concentration and size-resolved PN concentration at a traffic exposed site; and (iii) study the contribution of primary emission and secondary formation particles to the total urban PN concentration.

## 2. Materials and methods

### 2.1 Measurement sites

Measurements of particle number concentration and size distribution were performed at three different sites: a traffic exposed site (TR), an urban background site (UB), and a rural site (RU), located in the surroundings and

in the urban area of Piacenza, Italy. Piacenza is a mid-sized city with about 100,000 inhabitants located right in the middle of the Po Valley at about 60 m a.sl.. Despite its location in a context mostly rural and less urbanized compared with the largest metropolitan areas of the region, PM levels in Piacenza hardly comply with the air quality limits, especially as far as the PM10 daily limit is concerned (50 μg $m^{-3}$ as daily average, not to be exceeded more than 35 days in a year). The local Environmental Protection Agency reported non-attainment of the PM10 daily limit for Piacenza city centre from 2007 through 2014 and for the urban background site between 2010 and 2013 (annual number of exceedances in the 38-86 and 39-62 range, respectively); annual PM2.5 averages, measured only at this latter site, were in the 19-27 μg/$m^3$ range for the years 2010-2014, not in compliance with the 25 μg $m^{-3}$ limit only in 2011. According to its size and to the observed PM pollution levels, Piacenza can be regarded as a representative example of mid-sized cities in the Po valley.
Figure 1 gives an overview of the position of the three measurement sites. The traffic exposed site (TR: 45.056570° N, 9.706234° E) is located on the North-Eastern outskirts of Piacenza between the bank of the Po river and the motorway flyover (about 10 m above ground level) that borders the urban area at the North side. Aligned with the West-East direction, the flyover splits the surroundings of TR site into two main sectors: the Northern quadrants, where the river Po flows surrounded by floodplain and agricultural areas, and the Southern quadrants, with the urban areas of the city on the South-Western side and the commercial and industrial area on the South-Eastern side. Daily traffic on the motorway is about 40000 vehicles on workdays (with 40% of heavy-duty diesel trucks) and 30000 vehicles on weekends, with a smaller share of trucks (23% on Saturdays, 11% on Sundays). The urban background site (UB: 45.037843N, 9.668790° E) is about 3.5 km South-West from TR site and is located in the middle of a 0.16 $km^2$ public park in a residential area at the South-Western outskirts of Piacenza urban area; the nearest road is at about 300 m from the monitoring site. The rural site (RU: 44.909986° N, 9.597761° E) is located at about 20 km South from Piacenza in the garden of a private house in a small village on the first hills of the Apennines at about 150 m a.sl..

### 2.2 Measurement periods and instrumentation

Measurement campaigns were performed during different periods (i.e. not in parallel) from April 2011 to November 2012 at the three sites. Particle number (PN) concentrations, resolved in 12 size classes in the 7 nm-10 μm size range, were measured using an ELPI (Electrical Low Pressure Impactor, ELPI™ - Dekati Ltd., Finland; for details on the operating principle refer to Marjamaki et al., 2005) that was displaced at the different sites. ELPI was positioned in an air conditioned cabin, with the sampling system inlet at about 2 meters above the ground, and operated at 10 L/min nominal flow rate. Size-resolved PN data were collected at 1-min time resolution and all PN data were first reported to 10-min time resolution and then hourly averages were computed. TR site was the main monitoring site with about 250 days of data collection; at UB and RU site monitoring was carried on for 80 and 50 days, respectively. For each site, data were analyzed for cold period (October-March) and warm period (April-September) separately. Moreover distinction between workdays (Monday-Friday), Saturday and Sunday (+ holidays) were made.
Concurrently with PN measurements, an intensive campaign for the measurement of equivalent black carbon concentration (EBC) using a Multi Angle Absorption Photometer (MAAP mod. 5012, Thermo Scientific, USA; for details on the operating principle refer to Petzold et al., 2005) was performed with a 5-min time resolution in September 2012 at the TR site. Following Petzold et al. (2013) in this paper we use the term equivalent black carbon (EBC) instead of black carbon (BC) as the absorption properties have been measured by an optical technique and a MAC value (i.e. the mass-specific absorption coefficient) of 6.6 $m^2$ $g^{-1}$ has been used to convert light absorption into mass concentration. MAAP data were corrected following the approach introduced by

Hyvärinen et al. (2013).
Meteorological and air quality data were obtained from the local Environmental Protection Agency (ARPA Emilia-Romagna) monitoring networks: air temperature and pressure, relative humidity, wind speed and prevailing direction, solar radiation and precipitation at 1-h resolution were measured at a monitoring station located in the urban area of Piacenza. Table 1 summarizes the meteorological and air quality conditions during the measurement periods at the three sites. The area is characterized by a well-defined seasonality of ambient air temperature and relative humidity; conversely, low wind speeds (monthly averages around 1-1.7 m $s^{-1}$) characterize the area throughout the entire year. PM2.5 daily averages were in the range 5-43 μg $m^{-3}$ during the warm period and in the range 5-150 μg $m^{-3}$ during the cold period. The poorly developed atmospheric mixing and high air pollutant emissions from anthropogenic sources like traffic and heating processes are regarded as the main drivers for PM pollution seasonal pattern in the Po valley (Bigi and Ghermandi, 2014) during the cold period.

### 2.3 Cluster analysis

Instead of investigating the features on PN data for each single size bin, in this study cluster analysis was applied to the size-resolved PN data in order to identify size intervals characterized by similar patterns. The cluster analysis is a statistical tool for data reduction aiming at group objects in terms of their similarity, so that the degree of association is stronger between members of the same cluster and weaker between members of different clusters (MacQueen 1967; Jain et al., 1999). Previous studies have shown that cluster analysis is suitable for applications to particle size distribution data (e.g. Charron and Harrison, 2003; Beddows et al., 2009; Dall'Osto et al., 2011).The hourly averaged PN data in the 12 size classes measured during all campaigns composed the N×M (N = 12 size-classified PN data and M = 8200 hourly averages) input matrix of the hierarchical clustering. In order to prevent bias due to widely varying scales of PN in the 12 size classes, each variable was expressed as Z-score. The hierarchical clustering was performed based on Euclidean distance as similarity metric and average linkage as agglomerative method. The clustering was performed using the k-means algorithm (Wegner et al., 2012; Hussein et al., 2014) and choosing the optimum number of clusters based on the maximization of Dunn index values. The Dunn index reports the compactness of each cluster and the separation between the clusters, which is the most useful parameter for this type of application (Beddows et al., 2009).

## 3. Results and discussions

### 3.1 Particle number concentration and size distribution

The cluster analysis was conducted using different agglomerative methods (such as single linkage and Ward's method) and also performed separately for the three sites. The classifications suggested by the different analyses were consistent with the result reported in Figure 2 and fractioned the total PN data ($PN_{7\text{-}10000}$) into six representative size clusters: 7 <d< 29 nm ($PN_{7\text{-}29}$), 29 <d< 95 nm ($PN_{29\text{-}95}$), 95 <d< 264 nm ($PN_{95\text{-}264}$), 264 <d< 2410 nm ($PN_{264\text{-}2410}$), 2410 <d< 4020nm ($PN_{2410\text{-}4020}$), and 4020 <d< 10000 nm ($PN_{4020\text{-}10000}$). However, the three latter clusters were considered together because of the negligible contribution of coarse particles in terms of PN and are hereafter regarded as cluster 4 ($PN_{264\text{-}10000}$). In addition, $PN_{7\text{-}95}$ were considered as a measure of ultrafine particles (UFP), in order to compare our results with other studies.
Average concentration values for the total PN data ($PN_{7\text{-}10000}$) and for the 4 size-clustered data at the three monitoring sites are summarized in Table 2 separately for the cold and warm period and for workdays,

Saturdays and Sundays. The seasonal variations are consistent at all the sites, with higher PN levels during the cold period, on the average about 1.1-1.6 times higher than in the warm period. This can be explained by combination of the higher emissions from domestic heating (namely including biomass burning) together with the unfavorable atmospheric dispersion conditions in the cold period, such as the lower mixing height and the stronger atmospheric stability typical of the Po valley; new particle formation via nucleation processes might provide an additional contribution to cold period PN levels, as dilution of vehicle exhaust with cold air promotes nucleation and condensation of condensable organic compounds (Kittelson, 1998; Shi and Harrison, 1999). Similar PN seasonal patterns of PN have been reported for several urban areas worldwide (e.g.: Wehner and Wiedensohler, 2003; Hussein et al., 2005; Sabaliauskas et al., 2012).

Higher PN levels characterize TR site compared with UB (up to 90%) and RU (up to 130%) site in any season and day of the week considered; in turn, average PN levels at UB site are 10%-40% higher than at RU site. The observed intersite PN ratios are consistent with other multi-sites studies, namely with those reporting ratios between urban traffic exposed sites and urban background sites in the 1.5-5 range (Cyris et al., 2008; Boogaard et al., 2010, 2011; Wang et al., 2010a). At TR site average $PN_{7\text{-}10000}$ is in the 8720-17200 $cm^{-3}$ range with the lowest levels on warm Sundays and the highest on cold workdays. The ratio of workdays to Sundays for $PN_{7\text{-}10000}$ average levels varies from 1.6 during cold period to 1.3 during warm period, thus reflecting the variation in traffic flow and composition on the motorway. The ratios are comparable to values reported for other urban areas (Jeong et al., 2006; Wang et al., 2010b). At UB site $PN_{7\text{-}10000}$ records average levels in the 6260-11240 $cm^{-3}$ range. The difference between workdays and Sundays is less evident respect to that at TR site, as urban traffic doesn't change as much as on the motorway; the workdays to Sundays ratio for $PN_{7\text{-}10000}$ is around 1.2 in the cold period and 1.1 in the warm period. However, on the cold period Saturdays average levels higher than on workdays are observed for $PN_{7\text{-}10000}$ and for UFPs in particular; additionally, the time patterns of PN concentrations is different from those of the workdays. This fact is likely due to the increased local traffic on Saturdays due to the commercial area in the neighborhood of the park; the stronger activity of domestic heating sources may also contribute. At RU site average $PN_{7\text{-}10000}$ is in the 5780-9180 $cm^{-3}$ range with a peculiar time pattern that doesn't show the morning peak but, conversely, a progressive rise of the PN levels up to a first peak on the late afternoon and to a second one (smaller) on the evening hours in the cold season. Such pattern is likely determined by domestic heating, mostly fuelled with wooden biomass, and cooking emissions, with local traffic playing a less relevant role compared with the urban area of Piacenza. This is also confirmed by the limited variation in PN levels between workdays and Sundays and by and the slightly higher PN levels that characterize Saturdays' on both the cold and warm period.

On average, the contribution of UFP ($PN_{7\text{-}95}$) to $PN_{7\text{-}10000}$ varies between 65-78% at TR site, 58-75% at UB and 56-78% at RU site (Table 2). The observed contributions are smaller than the European mean ratio of 76% reported by Putaud et al. (2010). Other studies have reported slightly higher values (70-90% range) for urban background and traffic exposed site in European urban areas (Rodriguez et al., 2007; Salma et al., 2011). The lower proportion of UFP in this study might due to the measured size cutoff from 7 nm.

Figure 3 reports the comparison of the average particle number size distribution (PNSD) at the three sites. Size-resolved average concentrations and related standard deviations are given in Tables SM 1-SM 3 of Supplementary Materials. At all sites PNSDs present two main detectable modes, one nucleation mode at about 20 nm and one in the Aitken mode at about 70 nm, and a visible increase in PN of particles larger than 100 nm from warm to cold period. Coherently with the cluster-resolved data of Table 2, the difference between workdays' and Sundays' PNSD is more pronounced at TR site for nucleation mode particles ($PN_{7\text{-}29}$). In particular, it is clear that the size distributions at TR site always exhibit a stronger nucleation mode, highlighting the influence of fresh vehicle emissions due to the closer proximity to roadside. Several studies

have observed the existence of a strong mode around 20 nm at traffic exposed sites (Charron and Harrison, 2003; Ketzel et al., 2004). This mode is found to increase in size with increasing distance from roadside due to dilution, condensation and coagulation process affecting nucleation mode particles (Zhu et al., 2002a, 2002b; Zhang et al., 2004; Pirjola et al., 2006). At TR site a strong increase in nucleation mode concentration between warm and cold workdays is observed. This behaviour could be related to the enhanced nucleation of vehicle exhaust at low temperature as previously observed in roadside studies (Wang et al., 2008).

### 3.2 Particle number daily patterns

The average daily patterns at the three sites for the four size clusters previously identified ($PN_{7\text{-}29}$, $PN_{29\text{-}95}$, $PN_{95\text{-}264}$, $PN_{264\text{-}10000}$) are presented in Figure 4 for the cold and warm period and for workdays, Saturdays and Sundays separately. At TR and UB sites, all size fractions generally follow the daily cycle observed for $PN_{7\text{-}10000}$. It is remarkable that the morning peaks of ultrafine particles ($PN_{7\text{-}29}$ + $PN_{29\text{-}95}$) are more pronounced than those of the larger particles, especially at TR site, and particularly accentuated during cold period workdays. This evidence well agrees with the typical PNSD of vehicle emission showing a bimodal shape with a main mode in the nucleation size range (dp<30nm) and a second mode composed by primary carbonaceous particles in the range 50-200 nm (as reviewed by Morawska et al., 2008). At the RU site the daily peaks are evident at noon time and in the late afternoon on workdays and Saturdays.
During the cold period the daily patterns of the four different size fractions record a lag in the occurrence of the evening peak that appears earlier for $PN_{7\text{-}29}$ and $PN_{29\text{-}95}$ than for $PN_{95\text{-}264}$ and $PN_{264\text{-}10000}$ at the TR and UB site (Figure 4), which is likely the effect of condensation and coagulation processes leading smaller particle to grow into larger ones. Shallow mixing layer and cold temperature may favour these processes on cold evenings. Evidence of strong condensation and coagulation processes during cold evenings and nights has been observed in other urban areas in Po Valley (Rodriguez et al., 2007; Bigi et al., 2012). During the warm period the concentration for all size fractions are lower and a peak of particles in the smallest size fraction ($PN_{7\text{-}29}$) at noon time is also recorded specially on Sundays at UB and RU sites. The presence of peaks in nucleation mode particles around noon has been observed during the warm period in several urban areas, mainly in those characterized by high solar radiation (e.g. Moore et al., 2007; Pey et al., 2008; Perez et al., 2010; Cheung et al., 2011). Studies have proved that these peaks are not correlated with traffic markers (e.g.: black carbon, carbon monoxide, nitrogen monoxide, aromatics VOCs, iso-pentane), therefore suggesting the secondary origin of these small particles formed via photochemical nucleation of gaseous precursor arising from traffic or other urban sources (Moore et al., 2007; Reche et al., 2011).

### 3.3 Particle number and black carbon at TR site

The role of traffic emission on PN concentration and size distribution at TR site has been highlighted in section 3.1. As black carbon (BC) is considered as an indicator of combustion related particles and in urban areas it is assumed as an accurate tracer of primary traffic emissions, we investigated the relationship between PN and EBC data concurrently collected and the TR site. Firstly, as wind is a dominant factor affecting pollutant concentrations in the near-road environment (Baldwin et al., 2015), we focused on the analysis of the polar plots for PN and EBC data (Figure 5). These plots, which relate concentrations to the wind speed and direction, point out the role of local sources, as high concentrations occur under fairly low wind speed. Furthermore, the highest PN and EBC concentration levels are mostly associated with the same wind conditions, namely Westerly winds blowing at 1-1.5 m $s^{-1}$, indicating that traffic emission from the Western stretch of highway and

the emissions from the urban area of Piacenza are the main sources responsible for PN and EBC concentrations at this site. Rather high PN and EBC levels are also associated to Easterly and South-Easterly weak winds, still as a consequence of the highway emissions but also to some industrial plants (a cement kiln, a 855 MW combined-cycle power plant fueled by natural gas, a waste incinerator) located on the Eastern outskirts of Piacenza; stronger Easterly winds (2-2.5 m $s^{-1}$) are associated with high PN levels but with low EBC concentration. For winds blowing from North-West to East, that is from the rural area North of the Po river, both PN and EBC display the lowest concentrations.
The relationship between PN and EBC concentration is further analyzed following the methodology described by Rodriguez and Cuevas (2007):

$$N1 = S1 \cdot EBC \quad (1)$$
$$N2 = PN - N1 \quad (2)$$

where N1 stands for the number concentration of "those aerosols directly emitted in the particle phase" and "those compounds nucleating immediately after the emission"; N2 is mainly representative of the number concentration of new particles formed during the dilution, cooling and mixing of the vehicle exhaust with the ambient air or formed in ambient air once the exhaust gas is fully diluted and mixed with the ambient air. In the EBC-PN scatter plots of Figure 6 concentration data are mostly comprised between a S1 slope, representing the minimum PN/EBC ratio, and a S2 slope representing the general trend of the upper border of the data. In particular, slope S1 is interpreted as the minimum number of primary particles arising from vehicle exhaust emissions per unit mass of EBC in ambient air. The observed increase of PN/EBC ratios from S1 up to reach a maximum S2 value is caused by enhancements in the new particle formation rates. However, we extend the definition of N1, N2 and S1, S2 to the four clusters of particles, being able not only to split the total PN into its two components but also the PN for the single size-related clusters. Thus, the total PN for cluster1 is split into its two components N11 (directly emitted particles) and N21 (particles formed in the atmosphere); similarly, PN data for the other clusters are split into N12 and N22, N13 and N23, N14 and N24 components.
Summary statistics of the PN/EBC ratios and S1 and S2 slope values (expressed as $10^6$ particles $ng^{-1}$ EBC) for the four size clusters, for UFPs and for all particles are reported in Table 3. PN vs. EBC scatter plots and related slopes are shown in Figure 6 for UFPs and for all particles; cluster-resolved PN vs. EBC scatter plots are shown in Supplementary Material Figure SM 1. For all the size ranges, the slope S1 is close to 1st percentile, whereas slope S2 is a bit higher than 99th percentile. The slope S1 calculated for UFPs ($PN_{7\text{-}95}$) is 1.22, that is 62% of the slope calculated for all PN data (1.96). The slopes S1 exhibit around 0.5 for cluster1 ($PN_{7\text{-}29}$), cluster2 ($PN_{29\text{-}95}$), and cluster3 ($PN_{95\text{-}264}$) and 0.09 for cluster4 ($PN_{264\text{-}10000}$): all these values can be regarded as the smallest "minimum number of particles directly entering the air per nanogram of EBC emitted by vehicle exhaust". The upper slope S2 exhibits 10.33 for UFP, which is 70% of the slope S2 for the all PN data (14.77). The slope S2 for cluster1 takes 78% of the S2 for UFPs, indicating that the enhancements in the new particle formation mostly concern nucleation mode (< 30 nm) particles, involving those species, mainly organic compounds and sulfuric acid, emitted by the vehicle exhausts (Casati et al., 2007).
The slope S1 and S2 for all PN in this study are much lower compared with studies in other European cities using the same approach described by Rodriguez and Cuevas (2007). Reche et al. (2011) reported values of S1 is 3.2 at Lugano, 3.6 at North Kensington and Bern, 2.9 at London, 5.1 at Barcelona, 8.7 in Huelva and 9.9 in Santa Cruz de Tenerife. Rodriguez et al. (2007) observed S1 = 4.69 and S2 = 15.43 in Barcelona, and S1 = 4.75, and S2 = 22.57 in Milan. Those two studies only calculate the relationship between total PN and EBC without studying size-resolved particles. As the EBC concentration levels observed in Piacenza are comparable to other

Southern European cities (Rodriguez et al., 2007; Reche et al., 2011), the lower values for S1 and S2 derive from lower PN levels. The use of instruments measuring PN concentration with different cut sizes is likely the main reason influencing the S1 and S2 results: indeed, the higher the minimum bound of the measurement size range the lower the PN concentration, thus resulting in lower PN/BC ratios and in a lower slope S1. In our study, the 7 nm-10 μm measurement range of ELPI might have missed counting nucleation mode particles.

### 3.4 Daily pattern of N1 and N2 components

Both the N1 and N2 components of the total PN exhibit morning and evening peaks at rush hour corresponding with EBC peaks (Figure 7). However, while N1 peaks are in the same order of magnitude, the N2 morning peak is about twice as high as in the evening. The lower temperatures during morning rush hour may be more favourable for N2 particle formation through particle condensation and nucleation during cooling and dilution of vehicle exhaust; indeed, several studies reported increasing presence of nucleation mode particles at traffic sites during cold mornings (Jeong et al., 2006; Wang et al., 2008) and compared with evening rush hours (Charron and Harrison 2003; Janhäll et al., 2006).

Looking at cluster-related N2 components, in Figure 8 we can see that the daily pattern of the N2 component remains fairly constant throughout the day for cluster 3 and 4 (i.e.: N23 and N24); conversely, it displays the typical pattern of traffic-related pollutants for cluster 1 and 2 (i.e.: N21 and N22). In particular, new particle formation mostly affects N21 concentrations, with morning (up to 8000 $cm^{-3}$) and evening peak (about 5000 $cm^{-3}$) almost 3 times higher than the corresponding N22 values. These N21 components can be particles formed in ambient air once the exhaust gas is fully diluted and mixed with the ambient air, remaining mostly in the nucleation mode range (< 30 nm).

However, component N21 also exhibits a detectable increase on the early afternoon, when EBC concentration is at its minimum level. This suggests the formation of new particles not strictly related with local traffic emissions. Nucleation processes have been observed also in urban areas under strong solar radiation conditions and especially under clean air conditions because of the scarce pre-existing surface available for condensation of semi-volatile compounds (Rodriguez et al., 2005; Rodriguez et al., 2007; Shi et al., 2007; Salma et al., 2011). Actually, the analysis of the diurnal patterns of $PN_{7\text{-}29}$ and N21 components stratified for low-pollution days (PM2.5 daily average < 25th percentile of warm period PM2.5 daily averages, i.e.: PM2.5 < 11μg $m^{-3}$), mid-pollution days (PM2.5 daily average within the interquartile range, i.e.: 11 μg $m^{-3}$ < PM2.5 < 21 μg $m^{-3}$) and high-pollution days (PM2.5 daily average > 75th percentile, i.e.: PM2.5 > 21 μg $m^{-3}$) confirms that $PN_{7\text{-}29}$ levels during the early afternoon were higher on low- and mid-pollution days rather than on high-pollution days, consistently with the findings of the cited studies.

Cluster-resolved polar plots for the N1 and N2 components are shown in Figure 9 and 10, respectively: cluster-resolved plots for the total PN are shown in Supplementary material Figure SM 2.

Coherently with eq. (1), the polar plots for the N1 components mirror the EBC polar plot, with the highest concentration levels mostly associated with weak winds blowing form the Southern quadrants and along the East-West direction, especially for N11 and N12 particles; this confirms that the primary emissions from heavy-duty traffic along the motorway together with urban traffic emissions Southern of the TR site are the main sources for UFPs. Conversely, the concentrations of N14 particles, do not show dependency on wind direction and speed and, accordingly with the S1 slope values reported in Table 3, are about 5-6 times lower than those of the other clusters. Regardless for the size cluster, the lowest concentrations of N1 particles are associated with Northern and North-Easterly winds (i.e: blowing from the agricultural area).

Polar plots for the newly formed particles (Figure 10) show a weak dependency on wind direction and speed for

N22 particles and almost no dependency for larger-sized N23 and N24 particles. On the contrary, for nucleation mode particles N21 the polar plot, together with generally higher concentration levels, clearly highlights the association with wind conditions: indeed, the highest concentrations, in the order of 6000 $cm^{-3}$, are uniquely associated to South-Westerly and Westerly winds blowing at 1-1.5 m $s^{-1}$. Such wind conditions, coupled with a still shallow boundary layer, systematically occurred, thus confirming that most of the newly formed particles derive from nucleation processes after dilution, cooling and ambient air mixing of vehicle exhaust gas blown towards the TR site during the morning rush hours. This evidence is further confirmed by Sunday morning data: indeed, N21 concentrations between 6 and 9 AM were 2-3 times lower than on weekdays under the same wind conditions and up to 8-9 times lower under Easterly winds, that is winds blowing from the less urbanized areas.

## 4. Conclusions

Particle number concentration were measured at a traffic exposed and at an urban background site in the mid-sized city of Piacenza in the Po valley; measurements were also performed at a small village in the rural area about 20 km from Piacenza. Concentration levels in Piacenza are in substantial agreement with those measured at the largest cities of the Po valley, thus confirming the regional extent of air pollution issues as for PM mass concentration. Traffic intensity, atmospheric mixing height diurnal variation, and seasonality are the main drivers for the daily pattern of particle concentration. However, in the urban environments domestic heating and local traffic conditions can alter the typical traffic-driven pattern, as shown by Saturdays' data in our study. Size-resolved analysis pointed out four representative size clusters (7 <d< 29 nm, 29 <d< 95 nm, 95 <d< 264 nm, and 264 <d< 10000 nm), with ultrafine particles accounting for 55%-78% of the total particle number, depending on site, season and day on the week.

The daily patterns of the concentration recorded at the traffic site, both for the total particle number and for size-segregated clusters, follow the pattern of black carbon, once again confirming the main role of traffic as a particle source, especially as far as the smaller size clusters are concerned. The split between directly emitted and newly formed particles shows that the former are in the 7-264 nm size range, while the latter are almost exclusively in the nucleation mode size range (7-29 nm). Most of the newly formed particles derive from formation processes during/after dilution, cooling and ambient air mixing of vehicle exhaust gas during the morning rush hours. However, the increase in particle number observed on the early afternoon, when black carbon is at its minimum levels, suggests the occurrence of other new particle formation events that mainly involve particles in the nucleation mode size range. As the daily pattern of directly emitted particles closely follows black carbon, the trend of newly formed particles varies according to air temperature, solar radiation, wind conditions, and particle pollution levels; in particular, new particle formation events, affecting only the size range of ultrafine particles, were more intense under clean air conditions, that is when PM2.5 was below 10 μg $m^{-3}$ and the condensation sink is less relevant.

These results show that in the Po valley, even at traffic exposed sites, the daily variations of particle number levels might not always reflect the variation of road traffic emissions and related primary particles; indeed, the large availability of anthropogenic precursors in the Po valley can favor summertime nucleation events with region-wide extension. As reported by Decesari et al., (2014) the new particle formation events can be expected to frequently occur at rural locations (i.e., most parts of the Po valley). Nevertheless, they can be expected also at background sites in mid-sized and large urban areas where the decrease in particulate matter levels observed in recent years reduced the strength of the condensation sink. Without any appreciable change in gaseous precursors (e.g., aromatic VOCs and ammonia), still largely available because of the widespread agricultural activities and the weak air circulation, the frequency of new particle formation events in urban areas may

prospectively increase, influencing the daily concentration pattern and the exposure to ultrafine particles in the urban environment.

**Acknowledgements**

The financial support by Fondazione di Piacenza e Vigevano and Politecnico di Milano international fellowship grant are acknowledged. We also acknowledge the authors of the open source R programme. (R Core Team, 2015).

**References**

Baldwin, N., Gilani, O., Raja, S., Batterman, S., Ganguly, R., Hopke, P., Nichole, V., Robins, T., Hoogterp, S., 2015. Factors affecting pollutant concentrations in the near-road environment, Atmos. Environ. 115, 223-235.

Ban-Weiss, G.A., McLaughlin, J.P., Harley, R.A., Lunden, M.M., Kirchstetter, T.W., Kean, A.J., Strawa, A.W., Stevenson, E.D., Kendall, G.R., 2008. Long-term changes in emissions of nitrogen oxides and particulate matter from on-road gasoline and diesel vehicles. Atmos. Environ. 42, 220-232.

Beddows, D.C.S., Dall'Osto, M., Harrison, R.M., 2009. Cluster analysis of rural, urban, and curbside atmospheric particle size data. Environ. Sci. Tech. 43, 4694-4700.

Bernardoni, V., Vecchi, R., Valli, G., Piazzalunga, A., Fermo, P., 2011. PM10 source apportionment in Milan (Italy) using time-resolved data. Sci. Tot. Environ. 409, 4788-4795.

Bigi, A., Ghermandi, G., Harrison, R.M., 2012. Analysis of the air pollution climate at a background site in the Po valley. J Environ Monit. 14, 552-563

Bigi, A., Ghermandi, G., 2014. Long-term trend and variability of atmospheric PM10 concentration in the Po Valley. Atmos. Chem. Phys. 14, 4895-4907

Boogaard, H., Montagne, D., Brandenburger, A., Meliefste, K., Hoek, G., 2010. Comparison of short-term exposure to particle number, PM10 and soot concentrations on three (sub) urban locations. Sci. Total Environ. 408, 4403-4411.

Boogaard, H., Kos, G.P.A., Weijers E.P., Janssen, N.A.H, Fischer, P.H. et al. 2010. Contrast in air pollution components between major streets and background locations: Particulate matter mass, black carbon, elemental composition, nitrogen oxide and ultrafine particle number. Atmos. Environ. 45, 650-658.

Carslaw, D.C., Ropkins, K., 2012. Openair - an R package for air quality data analysis. Environmental Modelling & Software 27-28, 52-61.

Carslaw, D.C., 2015. The openair manual-open-source tools for analyzing air pollution data. Manual for version 1.1-4, King's College London.

Casati, R., Scheer, V., Vogt, R., Benter, T., 2007. Measurement of nucleation and soot mode particle emission from a diesel passenger car in real and laboratory in situ dilution. Atmos. Environ. 41, 2125-2135.

Charron, A., Harrison, R.M., 2003. Primary particle formation from vehicle emissions during exhaust dilution in the roadside atmosphere. Atmos. Environ. 37, 4109-4119.

Chio, C.P., Liao, C.-M., 2008. Assessment of atmospheric ultrafine carbon particle-induced human health risk based on surface area dosimetry. Atmos. Environ. 42, 8575-8584.

Cheung, H.C., Morawska, L., Ristovski, Z.D., 2011. Observation of new particle formation in subtropical urban environment. Atmos. Chem. Phys. 11, 3823-3833.

Cyrys, J., Pitz, M., Heinrich, J., Wichmann H-E., Peters A., 2008. Spatial and temporal variation of particle number concentration in Augsburg, Germany. Sci. Total Environ. 401, 168-175.

Dall'Osto, M., Monahan, C., Greaney, R., Beddows, D.C.S., Harrison, R.M., Ceburnis, D., O'Dowd, C.D.,

2011. A statistical analysis of North East Atlantic (submicron) aerosol size distributions, Atmos. Chem. Phys. 11, 12567-12578.

Decesari, S., Facchini, M.C., Rinaldi, M., Marinoni, A., Gobbi, G.P., Laaksonen, A., Manninen, H., Maione, M., Cavalli, F., Poluzzi, V., 2014. Ground-based observations of new particle formation during the summer 2012 PEGASOS - SUPERSITO field campaign in the Po Valley. Proceedings of EGU General Assembly Conference, Geophysical Research Abstracts, 6, EGU2014-7382.

Dunn, M.J., Jimenez, J.L., Baumgardner, D., Castro, T., Mc-Murry, P.H., Smith, J.N., 2004. Measurements of Mexico City nanoparticle size distributions: Observations of new particle formation and growth. Geophys. Res. Lett. 31, L10102.

EU Directive 2008/50/EC of the European Parliament and of the Council of 21 May 2008 on ambient air quality and cleaner air for Europe, Official Journal L 152, 11.6.2008, 1-44

Fernandez-Camacho, R., Rodrıguez, S., de la Rosa, J., Sanchez de la Campa, A.M., Viana, M., Alastuey, A., Querol, X., 2010. Ultrafine particle formation in the inland sea breeze airflow in Southwest Europe, Atmos. Chem. Phys. 10, 9615-9630.

Fuzzi, S., Baltensperger, U., Carslaw, K., Decesari, S., Denier van der Gon, H., Facchini, M.C., Fowler, D., Koren, I., Langford, B., Lohmann, U., Nemitz, E., Pandis, S., Riipinen, I., Rudich, Y., Schaap, M., Slowik, J.G., Spracklen, D.V., Vignati, E., Wild, M., Williams, M., Gilardoni, S., 2015. Particulate matter, air quality and climate: lessons learned and future needs. Atmos. Chem. Phys. 15, 8217-8299

Hoek G., Boogaard H., Knol A., de Hartog J., Slottje P., Ayres J.G., Borm P., Brunekreef B., Donaldson K., Forastiere F., Holgate S., Kreyling W.G., Nemery B., Pekkanen J., Stone V., Wichmann H.E., van der Sluijs J., 2010. Concentration response functions for ultrafine particles and all-cause mortality and hospital admissions: results of a European expert panel elicitation. Environ. Sci. Technol. 44, 476-482.

Hussein, T., Hämeri, K., Aalto, P.P., Kulmala, M., 2005. Modal structure and spatial-temporal variations of urban and suburban aerosols in Helsinki area. Atmos. Environ. 39, 1655-1668.

Hussein, T., Martikainen, J., Junninen, H., Soghaceva, L., Wagner, R., Dal Maso, M., Riipinen, I., Aalto, P.P., Kulmala, M., 2008. Observation of regional new particle formation in the urban atmosphere. Tellus B 60, 509-521.

Hussein, T., Mølgaard, B., Hannuniemi, H., Martikainen, J., Järvi, L., Wegner, T., Ripamonti, G., Weber, S., Vesala, T., Hämeri, K., 2014. Finger-printing the Urban Particle Number Size Distribution in Helsinki, Finland: Local versus regional characteristics. Boreal Env. Res. 19, 1-20.

Hyvärinen, A.-P., Vakkari, V., Laakso, L., Hooda, R.K, Sharma, V. P., Panwar, T.S., Beukes, J.P., van Zyl, P., Josipovic, M., Garland, R.M., Andreae, M.O., Pöschl, U., Petzold, A., 2013. Correction for a measurement artifact of the Multi-Angle Absorption Photometer (MAAP) at high black carbon mass concentration levels. Atmos. Meas. Tech. 6, 81-90.

Janhäll, S., Olofson, F., Andersson, P., Pettersson, J., Hallquist, M., 2006. Evolution of the Urban Aerosol During Winter Temperature Inversion Episodes. Atmos. Environ. 40, 5355-5366.

Jain, A.K., Murty, M.N., Flynn, P.J., 1999. Data Clustering: A Review. ACM Computer Survey 31, 264-323.

Jamriska, M., Morawska, L., Mergersen, K., 2008. The effect of temperature and humidity on size segregated traffic exhaust particle emissions. Atmos. Environ. 42, 2369-2382

Janssen, N.A.H., Gerlofs-Nijland, M.E., Lanki, T., Salonen, R.O., Cassee, F., Hoek, G., Fischer, P., Brunekreef, B., Krzyzanowski, M., 2012. Health Effects of Black Carbon. World Health Organization, Regional office for Europe

Jeong, C.-H., Evans, G., Hopke, P., Chalupa, D., Utell, M., 2006. Influence of atmospheric dispersion and new particle formation events on ambient particle number concentration. J. Air Waste Manage. Assoc. 56,

431-443.
Jonsson, Å.M., Westerlund, J., Hällquist, M., 2011. Size-resolved particle emission factors for individual ships. Geophys. Res. Let. 38, L13809.
Ketzel, M., Wåhlin, P., Kristensson, A., Swietlicki, E., Berkowicz, R., Nielsen, O.J., Palmgren, F., 2004. Particle size distribution and particle mass measurements at urban, near-city and rural level in the Copenhagen area and Southern Sweden. Atmos. Chem. Phys. 4, 281-292.
Kittelson, D.B., 1998. Engines and nanoparticles: a review. J. Aerosol Sci. 29, 575-588.
Kittelson, D.B., Watts, W. F., Johnson, J., 2002. Diesel Aerosol Sampling Methodology - CRC E-43: Final Report, University of Minnesota, Report for the Coordinating Research Council.
Kittelson, D.B., Watts, W.F., Johnson, J.P., 2006. On-road and laboratory evaluation of combustion aerosols e part 1: summary of diesel engine results. J. Aerosol Sci. 37, 913-930.
Kulmala, M., Vehkamäki, H., Petäjä, T., Dal Maso, M., Lauri, A., Kerminen, V.-M., Birmili, W., McMurry, P., 2004. Formation and growth rates of ultrafine atmospheric particles: a review of observations. J. Aerosol Sci. 35, 143-176.
Kumar, P., Robins, A., Vardoulakis, S., Britter, R., 2010. A review of the characteristics of nanoparticles in the urban atmosphere and the prospects for developing regulatory control. Atmos. Environ. 44, 5035-5052.
Lonati, G., Crippa, M., Gianelle, V., Van Dingenen, R., 2011. Daily patterns of the multi-modal structure of the particle number size distribution in Milan, Italy. Atmos. Environ. 45, 2434-2442.
MacQueen, J.B., 1967. Some Methods for Classification and Analysis of Multivariate Observations. Proceedings of 5th Berkeley Symposium on Mathematical Statistics and Probability, Berkeley, University of California Press 1, 281-297.
Marjamäki, M., Lemmetty, M., Keskinen, J., 2005. ELPI Response and Data Reduction I: Response Functions. Aerosol Sci. Technol. 39, 575-582.
Moore, K.F., Ning, Z., Ntziachristos, L., Schauer, J.J., Sioutas, C., 2007. Daily variation in the properties of urban ultrafine aerosol- Part I: Physical characterization and volatility. Atmos. Environ. 41, 8633-8646.
Morawska, L., Ristovski, Z., Jayaratne, R., Keogh, D. U., Ling, X., 2008. Ambient nano and ultrafine particles from motor vehicle emissions: characteristics, ambient processing and implications on human exposure. Atmos. Environ. 42, 8113-8138.
Ozgen, S., Ripamonti, G., Malandrini, A., Ragettli, M.S., Lonati, G., 2016. Particle number and mass exposure concentrations by commuter transport modes in Milan, Italy. AIMS Environmental Science, 3, 168-184.
Perez, N., Pey, J., Cusack, M., Reche, C., Querol, X., Alastuey, A., Viana, M., 2010. Variability of particle number, black carbon, and PM(10), PM(2.5), and PM(1) levels and speciation: influence of road traffic emissions on urban air quality. Aerosol Sci. Technol. 44, 487-499.
Petzold, A., Schloesser, H., Sheridan, P.J., Arnott, P.W., Ogren, J.A., Virkkula, A., 2005. Evaluation of Multiangle Absorption Photometry for Measuring Aerosol Light Absorption. Aerosol Sci. Tech. 39, 40-51.
Petzold, A., Ogren, J.A., Flebig, M., Laj, P., Li, S.-M., Baltensperger, U., Holzer-Popp, T., Kinne, S., Pappalardo, G., Sugimoto, N., Wehrli, C., Wiedensohler, A., Zhang, X.-Y., 2013. Recommendations for reporting “black carbon” measurements. Atmos. Chem. Phys. 13, 8365-8379.
Pey, J., Rodriguez, S., Querol, X., Alastuey, A., Moreno, T., Putaud, J.P., Van Dingenen, R., 2008. Variations of urban aerosols in the western Mediterranean. Atmos. Environ. 42, 9052-9062.
Pey, J., Querol, X., Alastuey, A., Rodrıguez, S., Putaud, J.P., Van Dingenen, R., 2009. Source apportionment of urban fine and ultrafine particle number concentration in a Western Mediterranean city. Atmos. Environ. 43, 4407-4415.
Pirjola, I., Paasonen, P., Pfeiffer, D., Hussein, T., Hameri, K., Koskentalo, T., Virtanen, A., Ronkko, T.,

Keskinen, J., Pakkanen, T., Hillamo, R., 2006. Dispersion of Particles and Trace Gases Nearby a City Highway: Mobile Laboratory Measurements in Finland. Atmos. Environ. 40, 867-879.

Putaud, J-P., Van Dingenen, R., Alastuey, A., Bauer H., Birmili W., et al., 2010. A European aerosol phenomenology 3: Physical and chemical characteristics of particulate matter from 60 rural, urban, and kerbside sites across Europe. Atmos. Environ. 44, 1308-1320.

Ramanathan, V., Carmichael, G., 2008. Global and regional climate changes due to black carbon. Nature geoscience. 1, 221-227.

R Core Team, 2015. R: A language and environment for statistical computing. R Foundation for Statistical Computing, Vienna, Austria. URL http://www.R-project.org/.

Reche, C., Querol, X., Alastuey, A., Viana, M., Pey, J., Moreno, T., Rodriguez, S., Gonzalez, Y., Fernandez-Camacho, R., de la Rosa, J., Dall'Osto, M., Prevot, A.S.H., Hueglin, C., Harrison, R.M., Quincey, P., 2011. New considerations for PM, Black Carbon and particle number concentration for air quality monitoring across different European cities. Atmos. Chem. Phys. 11, 6207-6227.

Ristovski, Z., Jayaratne, E.R., Lim, M., Ayoko, G.A., Morawska, L., 2006. Influence of diesel fuel sulphur on the nanoparticle emissions from city buses. Environ. Sci. & Tech. 40, 1314-1320

Rodriguez, S., van Dingenen, R., Putaud, J., Martins-Dos Santos, S., Roselli, D., 2005. Nucleation and growth of new particles in the rural atmosphere of Northern Italy - Relationship to air quality monitoring. Atmos. Environ. 39, 6734-6746.

Rodriguez, S., Cuevas, E., 2007. The contributions of "minimum primary emissions" and "new particle formation enhancements" to the particle number concentration in urban air. J. Aerosol Sci. 38, 1207-1219

Rodriguez, S., Van Dingenen, R., Putaud, J. P., Dell'Acqua, A., Pey, J., Querol, X., Alastuey, A., Chenery, S., Ho, K.-F., Harrison, R., Tardivo, R., Scarnato, B., Gemelli, V., 2007. A study on the relationship between mass concentrations, chemistry and number size distribution of urban fine aerosols in Milan, Barcelona and London. Atmos. Chem. Phys. 7, 2217-2232.

Ronkko, T., Virtanen, A., Vaaraslahti, K., Koskinen, J., Pirjola, L., Lappi, M., 2006. Effect of dilution conditions and driving parameters on nucleation mode particles in diesel exhaust: Laboratory and on-road study. Atmos. Environ. 40, 2893-2901.

Sabaliauskas, K., Jeong, C.H., Yao, X., Jun, Y-S., Jadidian, P., Evans, G.J., 2012. Five-year roadside measurements of ultrafine particles in a major Canadian city. Atmos. Environ. 49, 245-256.

Salma, I, Borsós, T, Weidinger, T, Aalto, P.P., Hussein, T, Kulmala, M., 2011. Production, growth and properties of ultrafine atmospheric aerosol particles in an urban environment. Atmos. Chem. Phys. 11, 1339-1353.

Shi, P.J., Harrison, R.M., 1999. Investigation of ultrafine particle formation during diesel exhaust dilution. Environ. Sci. Technol. 33, 3730-3736.

Shi Zong-bo, He Ke-bin, Xue-chun, Y., Zhi-liang, Y., Fu-mo, Y., et al., 2007 Diurnal variation of number concentration and size distribution of ultrafine particles in the urban atmosphere of Beijing in winter. J. Environ. Sci. 19, 933-938.

Sioutas, C., Delfino, R. J., Singh, M., 2005. Exposure assessment for atmospheric ultrafine particles (UFP) and implications in epidemiological research. Environ. Health Perspect. 113, 947-955.

Vecchi, R., Marcazzan, G., Valli, G., Ceriani, M., Antoniazzi, C., 2004. The role of atmospheric dispersion in the seasonal variation of PM1 and PM2.5 concentration and composition in the urban area of Milan (Italy), Atmos. Environ. 38, 4437-4446.

Vecchi, R., Bernardoni, V., Fermo, P., Lucarelli, F., Mazzei, F., Nava, S., Piazzalunga, A., Prati, P., Valli, G., 2009. 4-hours resolution data to study PM10 in a "hot spot" area in Europe. Environ. Monit. Assess. 154, 283-300.

Wang, F., Ketzel, M., Ellermann, T., Wåhlin, P., Jensen, S., Fang, D., Massling, A., 2010a. Particle number, particle mass and $NO_x$ emission factors at a highway and an urban street in Copenhagen. Atmos. Chem. Phys. 10, 2745-2764.

Wang, F., Costabile, F., Li, H., Fang, D., Allegrini, I., 2010b. Measurements of ultrafine particle size distribution near Rome. Atmos. Res. 98, 69-77

Wang, Y., Zhu, Y., Salinas, R., Ramirez, D., Karnae, S., John, K., 2008. Roadside measurements of ultrafine particles at a busy urban intersection. J. Air Waste Manage. Assoc. 58, 1449-1457.

Wang, Y., Hopke, P.K., Chalupa, D.C., Utell, M.J., 2011. Long-term study of urban ultrafine particles and other pollutants. Atmos. Environ. 45, 7672-7680.

Wegner, T., Hussein T., Hämeri K., Vesala T., Kulmala, M., Weber, S., 2012. Properties of aerosol signature size distributions in the urban environment as derived by cluster analysis. Atmos. Environ. 61, 350-360.

Wehner, B., Wiedensohler, A., 2003. Long term measurements of submicrometer urban aerosols: statistical analysis for correlations with meteorological conditions and trace gases. Atmos. Chem. Phys. 3, 867-879.

Zhang, K.M., Wexler, A.S., Zhu, Y.F., Hinds, W.C., Sioutas, C., 2004. Evolution of particle number distribution near roadways. Part II: the 'road-to-ambient' process. Atmos. Environ. 38, 6655-6665.

Zhu, Y.F., Hinds,W.C., Kim, S., Sioutas, C., 2002a. Concentration and size distribution of ultrafine particles near a major highway. J. Air Waste Manage. Assoc. 52, 1032-1042.

Zhu, Y., Hinds, W.C., Kim, S., Shen, S., Sioutas, C. 2002b. Study of ultrafine particles near a major highway with heavy-duty diesel traffic. Atmos. Environ. 36, 4323-4335.

## TABLES

Table 1 - Average meteorological and air quality conditions during the cold and warm measurement periods at the three sites (standard deviations in parentheses)

| Site | Season | Measurement periods (*) | $T_{air}$ (°C) | RH (%) | U ($m\ s^{-1}$) | $PM_{2.5}$ (**) ($\mu g\ m^{-3}$) |
|---|---|---|---|---|---|---|
| TR | cold | 2011: 10, 12<br>2012: 2-3 | 9.7 (6.6) | 74 (20) | 1.1 (0.7) | 37.2 (24.6) |
| | warm | 2011: 4-6, 9<br>2012: 4, 6-7 | 19.1 (6.9) | 63 (19) | 1.5 (0.9) | 16.9 (5.7) |
| UB | cold | 2011: 11 | 6.7 (4.5) | 88 (8) | 1.2 (1.0) | 32.3 (14.8) |
| | warm | 2011: 7, 9<br>2012: 5 | 20.6 (5.4) | 64 (18) | 1.4 (0.9) | 15.5 (5.8) |
| RU | cold | 2012: 11 | 8.9 (2.4) | 91 (9) | 1.2 (0.9) | 39.6 (16.8) |
| | warm | 2012: 9 | 19.9 (4.6) | 68 (19) | 1.3 (0.9) | 19.2 (9.4) |

(*) Year and month (Jan = 1); (**) PM2.5 data from UB site

Table 2 - Average and standard deviation of PN concentrations ($10^4$ $cm^{-3}$) at the three sites for cold and warm period and for workdays (Wo), Saturdays (Sa) and Sundays (Su). In the last row the UFP ($PN_{7-95}$) to total PN ($PN_{7-10000}$) ratio is given as a percentage.

| Size range | Parameter | TR SITE | | | | | | UB SITE | | | | | | RU SITE | | | | | |
|---|---|---|---|---|---|---|---|---|---|---|---|---|---|---|---|---|---|---|---|
| | | Cold Period | | | Warm period | | | Cold Period | | | Warm period | | | Cold Period | | | Warm period | | |
| | | Wo | Sa | Su | Wo | Sa | Su | Wo | Sa | Su | Wo | Sa | Su | Wo | Sa | Su | Wo | Sa | Su |
| $PN_{7-10000}$ | Avg. | 1.72 | 1.26 | 1.05 | 1.14 | 1.01 | 0.87 | 0.91 | 1.12 | 0.81 | 0.78 | 0.70 | 0.63 | 0.75 | 0.92 | 0.63 | 0.58 | 0.65 | 0.58 |
| | *St. dev.* | *1.06* | *0.58* | *0.44* | *0.56* | *0.45* | *0.35* | *0.55* | *0.47* | *0.53* | *0.43* | *0.29* | *0.27* | *0.59* | *0.54* | *0.24* | *0.27* | *0.22* | *0.19* |
| $PN_{7-29}$ | Avg. | 0.91 | 0.57 | 0.41 | 0.59 | 0.52 | 0.44 | 0.31 | 0.42 | 0.24 | 0.36 | 0.27 | 0.26 | 0.34 | 0.33 | 0.16 | 0.30 | 0.33 | 0.25 |
| | *St. dev.* | *0.58* | *0.41* | *0.27* | *0.42* | *0.36* | *0.27* | *0.19* | *0.21* | *0.28* | *0.27* | *0.26* | *0.17* | *0.28* | *0.23* | *0.11* | *0.19* | *0.26* | *0.12* |
| $PN_{29-95}$ | Avg. | 0.41 | 0.33 | 0.28 | 0.33 | 0.29 | 0.25 | 0.25 | 0.31 | 0.23 | 0.24 | 0.22 | 0.19 | 0.21 | 0.25 | 0.18 | 0.16 | 0.17 | 0.16 |
| | *St. dev.* | *0.25* | *0.16* | *0.12* | *0.18* | *0.14* | *0.10* | *0.15* | *0.15* | *0.17* | *0.10* | *0.08* | *0.08* | *0.11* | *0.17* | *0.08* | *0.06* | *0.05* | *0.05* |
| $PN_{95-264}$ | Avg. | 0.28 | 0.24 | 0.24 | 0.17 | 0.15 | 0.13 | 0.22 | 0.26 | 0.22 | 0.14 | 0.15 | 0.12 | 0.14 | 0.22 | 0.18 | 0.09 | 0.11 | 0.11 |
| | *St. dev.* | *0.13* | *0.11* | *0.11* | *0.08* | *0.07* | *0.06* | *0.10* | *0.06* | *0.07* | *0.04* | *0.05* | *0.06* | *0.06* | *0.07* | *0.03* | *0.02* | *0.03* | *0.04* |
| $PN_{264-10000}$ | Avg. | 0.12 | 0.12 | 0.13 | 0.05 | 0.05 | 0.05 | 0.13 | 0.13 | 0.13 | 0.04 | 0.05 | 0.04 | 0.06 | 0.11 | 0.10 | 0.03 | 0.04 | 0.05 |
| | *St. dev.* | *0.07* | *0.06* | *0.07* | *0.02* | *0.03* | *0.02* | *0.07* | *0.03* | *0.03* | *0.02* | *0.03* | *0.03* | *0.03* | *0.04* | *0.01* | *0.01* | *0.02* | *0.03* |
| UFP/PN (%) | Avg. | 73 | 70 | 65 | 78 | 78 | 78 | 58 | 65 | 57 | 75 | 69 | 71 | 70 | 63 | 55 | 78 | 75 | 71 |
| | *St. dev.* | *9* | *8* | *7* | *9* | *9* | *8* | *7* | *9* | *12* | *11* | *9* | *12* | *9* | *9* | *12* | *12* | *10* | *12* |

Table 3 - Summary statistic of the PN/EBC ratios ($10^6$ particles $ng^{-1}$ EBC) for single size clusters, UFPs, and all particles: minimum (min), 1st, 2nd, 50th, 98th and 99th percentile, maximum (max), slope S1 and S2.

| Size range | min | 1st | 2nd | 50th | 98th | 99th | max | S1 | S2 |
|---|---|---|---|---|---|---|---|---|---|
| $PN_{7\text{-}29}$ | 0.37 | 0.55 | 0.63 | 1.76 | 5.14 | 5.73 | 7.85 | 0.48 | 7.82 |
| $PN_{29\text{-}95}$ | 0.50 | 0.58 | 0.61 | 1.01 | 2.74 | 3.16 | 4.55 | 0.55 | 4.51 |
| $PN_{95\text{-}264}$ | 0.29 | 0.43 | 0.45 | 0.64 | 1.52 | 1.76 | 2.53 | 0.41 | 2.50 |
| $PN_{264\text{-}10000}$ | 0.08 | 0.11 | 0.12 | 0.25 | 0.43 | 0.45 | 0.48 | 0.09 | 0.48 |
| UFP ($PN_{7\text{-}95}$) | 1.01 | 1.34 | 1.45 | 2.75 | 7.73 | 8.52 | 11.78 | 1.22 | 10.33 |
| All PN ($PN_{7\text{-}10000}$) | 1.60 | 1.87 | 1.98 | 3.23 | 9.43 | 10.33 | 14.62 | 1.96 | 14.62 |

#

## FIGURES

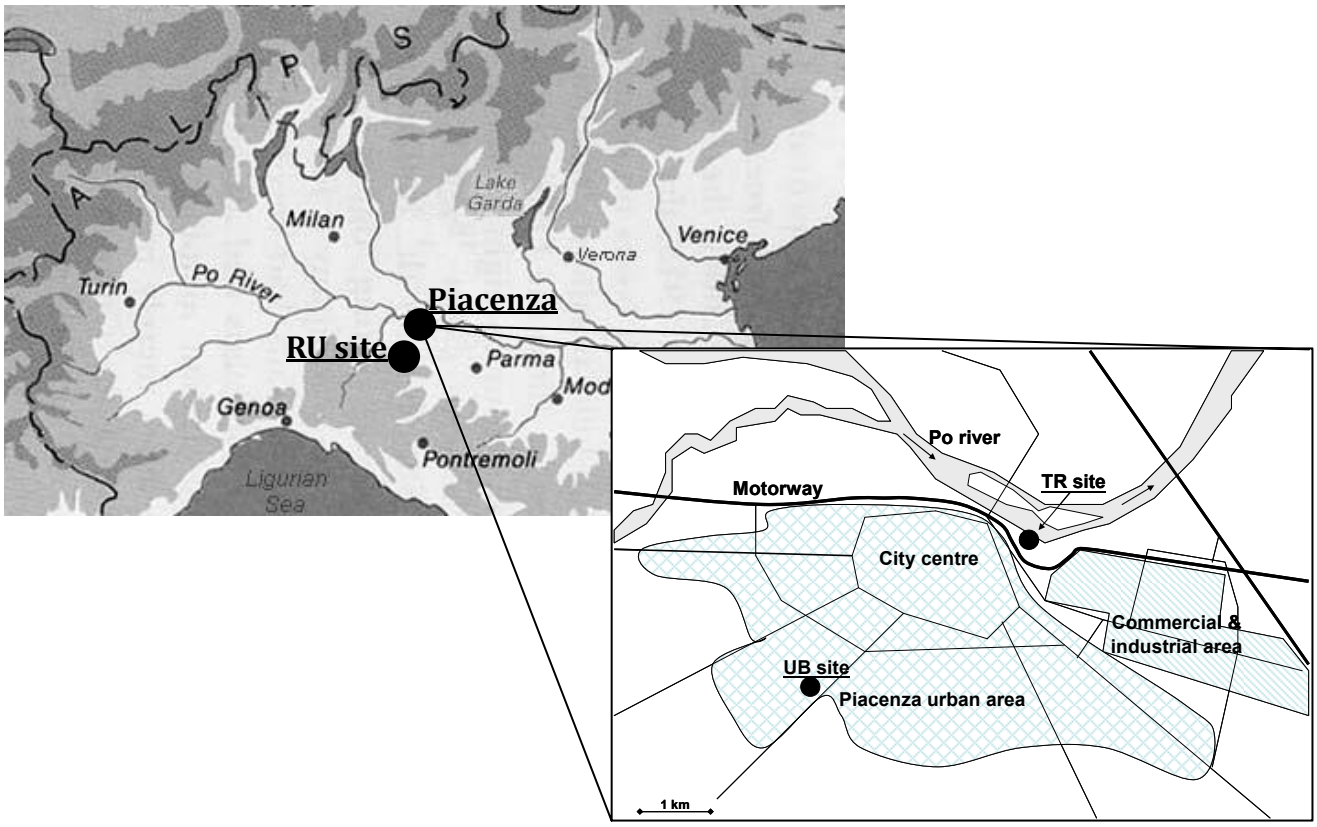


Figure 1 - Geographical localization of the three measurement sites: Traffic exposed site (TR), urban background site (UB) and rural site (RU).

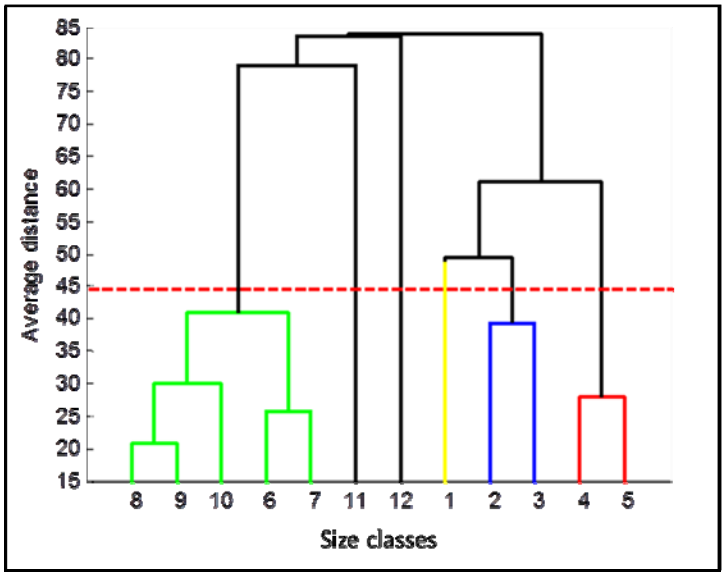


| Cluster | Size class | Size range (nm) |
|---|---|---|
| Cluster 1 | 1 | 7-29 |
| Cluster 2 | 2 | 29-57 |
| | 3 | 57-95 |
| Cluster 3 | 4 | 95-157 |
| | 5 | 157-264 |
| Cluster 4 | 6 | 264-384 |
| | 7 | 384-617 |
| | 8 | 617-954 |
| | 9 | 954-1610 |
| | 10 | 1610-2410 |
| | 11 | 2410-4020 |
| | 12 | 4020-10000 |

Figure 2 - Hierarchical clustering of the hourly averaged PN in the 12 size classes measured during all the campaigns.

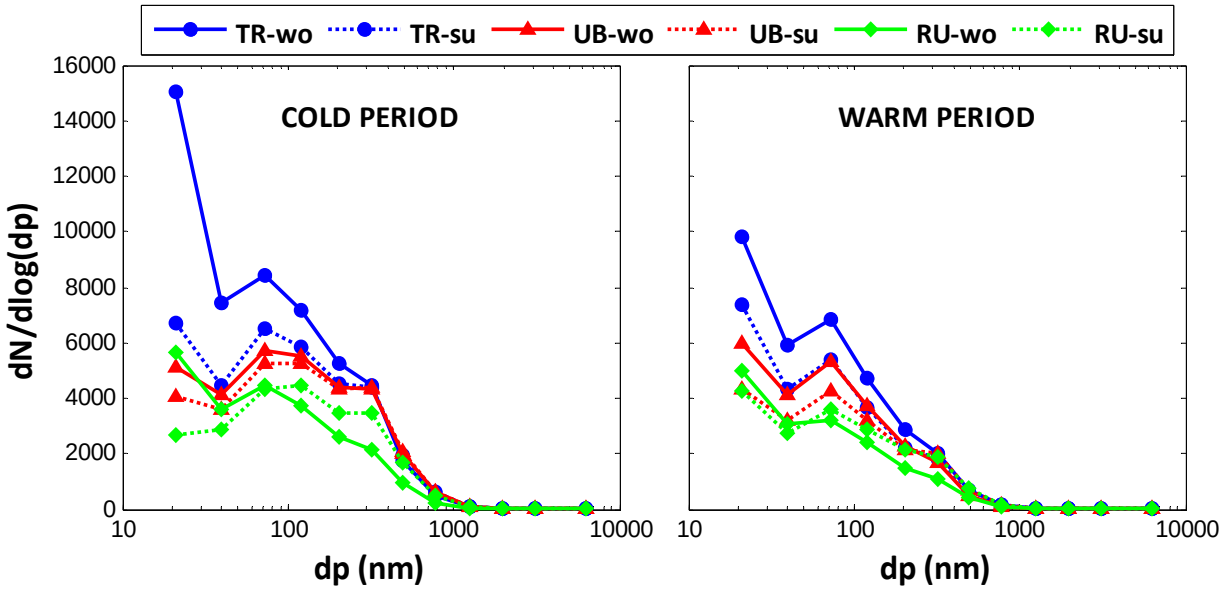


Figure 3 - Average workdays' and Sundays' PNSD at the three sites for the cold and warm period.

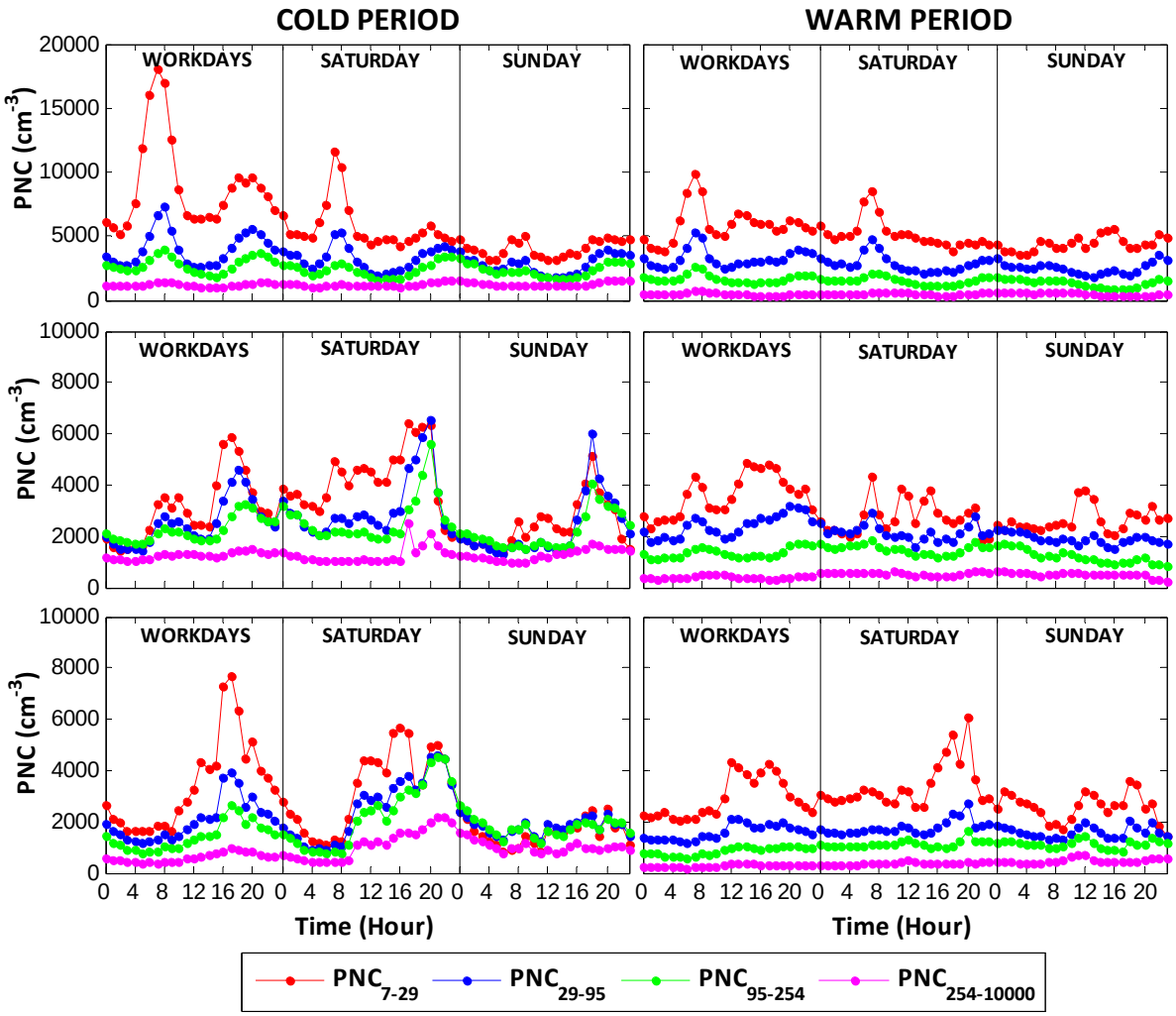


Figure 4 - Average daily pattern of the PNC for the four size clusters at the three sites for cold and warm period and workdays, Sundays and Saturdays. (Top panels: TR site; Middle panels; UB site; Bottom

panels: RU site)

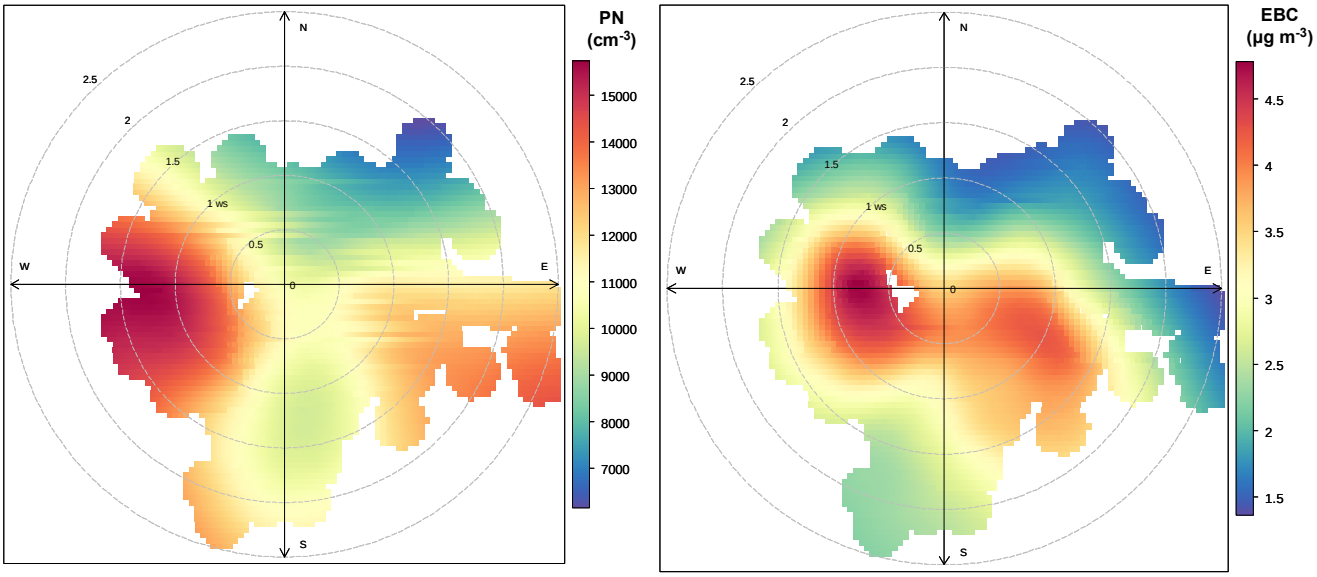


Figure 5 - Polar plots of particle number (PN, $cm^{-3}$, left panel) and equivalent black carbon (EBC, µg $m^{-3}$, right panel) concentrations associated with wind speed and wind direction, the color scale shows the pollutant concentrations and the radial scale shows the wind speed which increases radially outwards from the center. The graphs are generated using Openair in R programming (Carslaw and Ropkins, 2012; Carslaw, 2015).

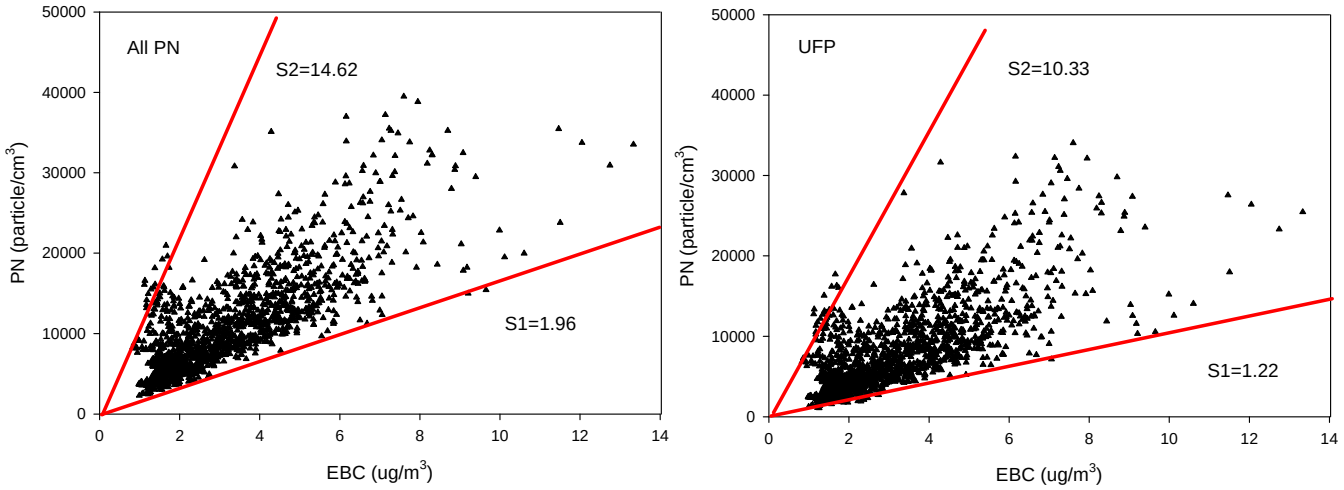


Figure 6 - PN vs EBC scatter plots at TR site for $PN_{7\text{-}10000}$ (all data, left panel) and $PN_{7\text{-}95}$ (UFP, right panel). S1 and S2 indicate the lines of the minimum and maximum slope that contain the most part of the

data.

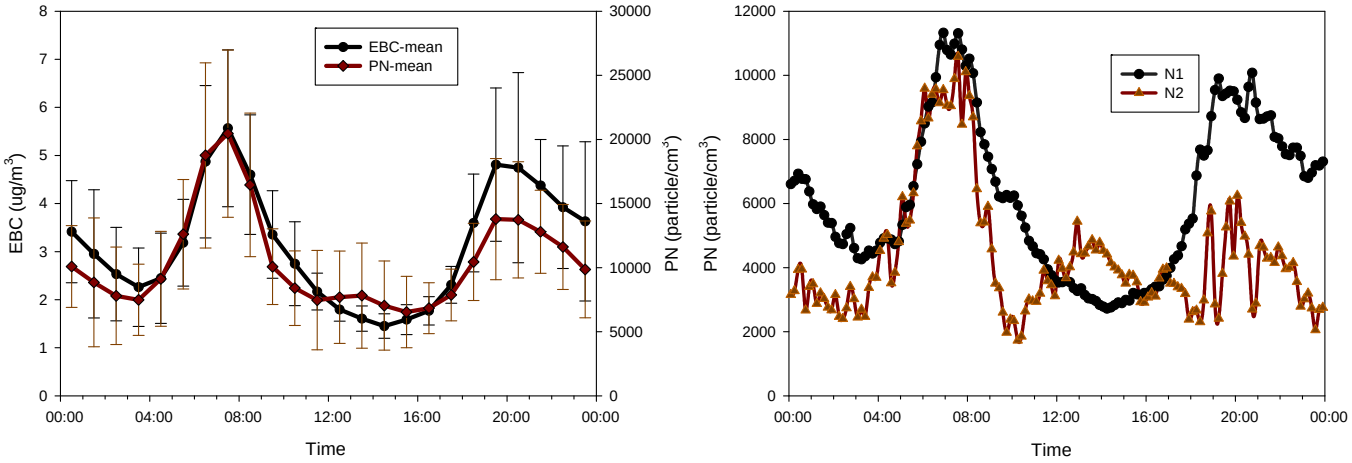


Figure 7 - Daily pattern of PN and EBC (left panel), N1 and N2 (right panel) at TR site.

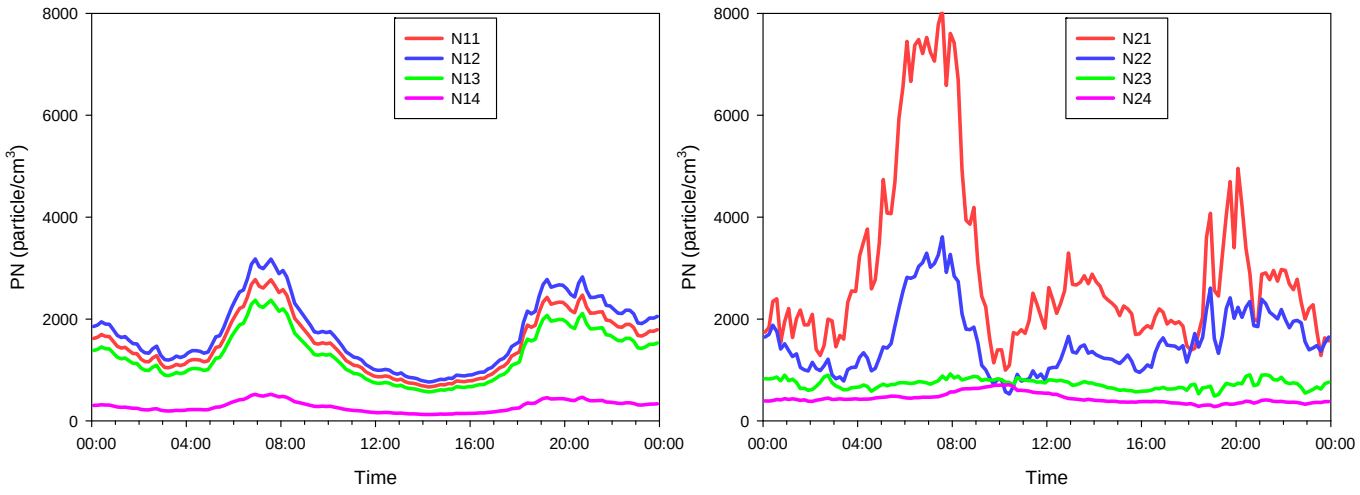


Figure 8 - Daily pattern of cluster-resolved N1 components (left panel) and N2 components (right panel) for the four size clusters at TR site.

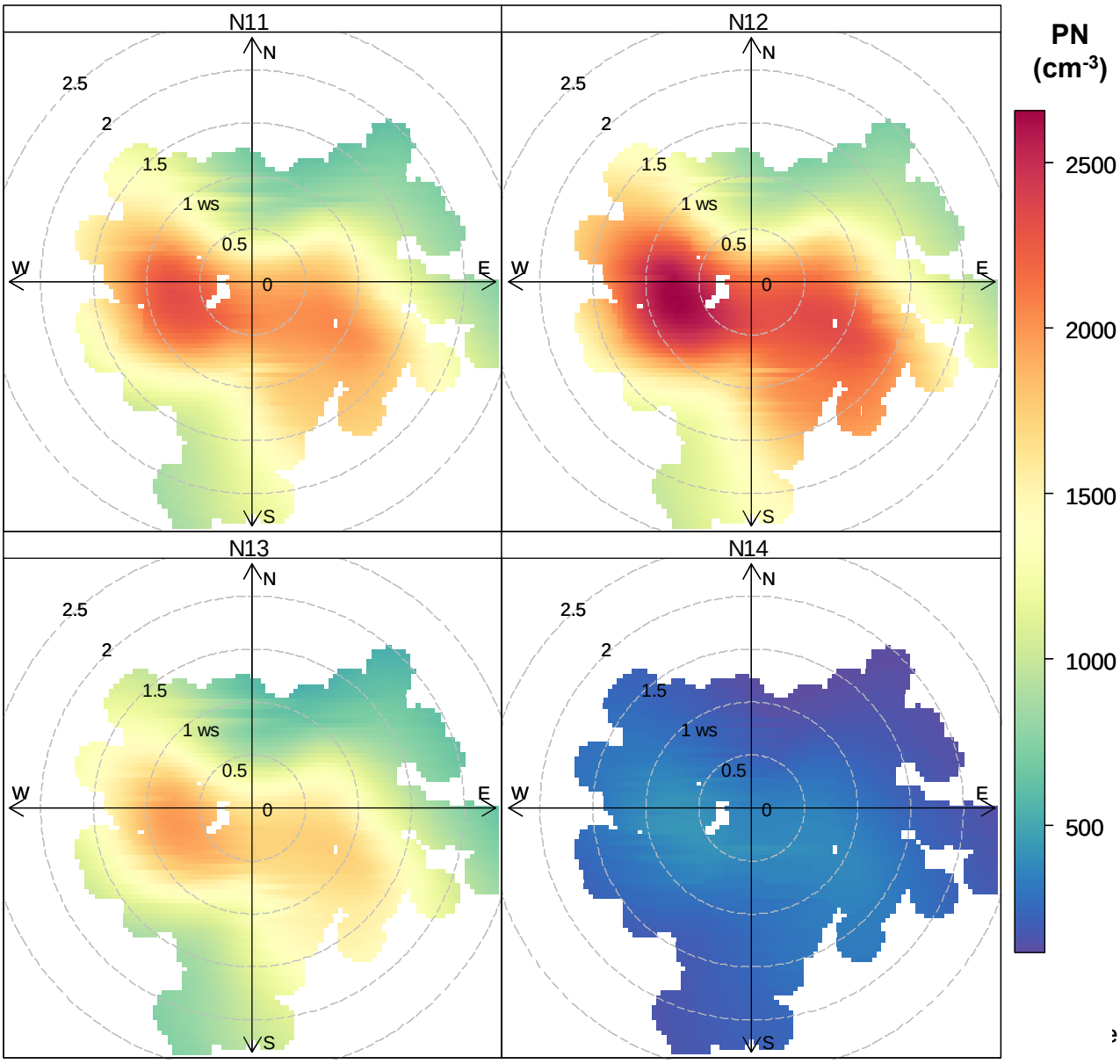


Figure 9 - Polar plots of N1 particles number concentrations (PN, $cm^{-3}$) for the four size clusters associated with wind speed and wind direction, the color scale shows the concentration and the radial scale shows the wind speed which increases radially outwards from the centre.

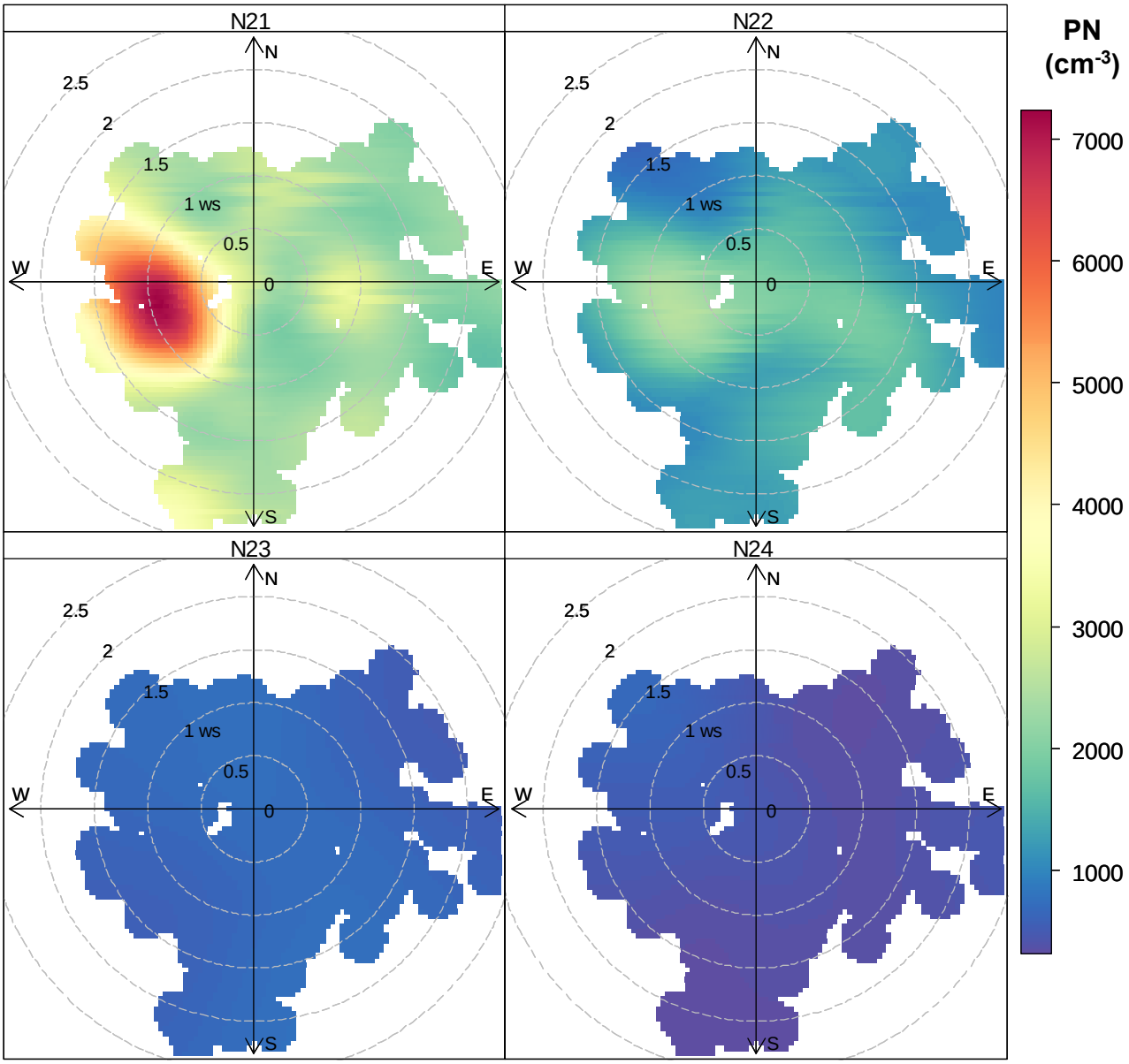


Figure 10 - Polar plots of N2 particles number concentrations (PN, $cm^{-3}$) for the four size clusters associated with wind speed and wind direction, the color scale shows the concentration and the radial scale shows the wind speed which increases radially outwards from the centre.